

Accepted Manuscript

Predictive Value of the OCT Double-Layer Sign for Identifying Subclinical Neovascularization in Age-Related Macular Degeneration

Yingying Shi, MD, Elie H. Motulsky, MD, PhD, Raquel Goldhardt, MD, FACS, Yehoshua Zohar, MD, MHA, Marie Thulliez, MD, William Feuer, MS, Giovanni Gregori, PhD, Philip J. Rosenfeld, MD, PhD

PII: S2468-6530(18)30495-0

DOI: <https://doi.org/10.1016/j.oret.2018.10.012>

Reference: ORET 419

To appear in: *Ophthalmology Retina*

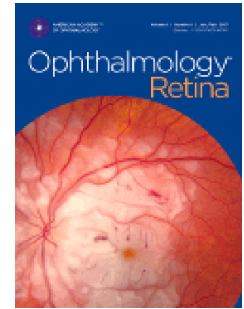
Received Date: 8 August 2018

Revised Date: 15 October 2018

Accepted Date: 19 October 2018

Please cite this article as: Shi Y., Motulsky E.H., Goldhardt R., Zohar Y., Thulliez M., Feuer W., Gregori G. & Rosenfeld P.J., Predictive Value of the OCT Double-Layer Sign for Identifying Subclinical Neovascularization in Age-Related Macular Degeneration, *Ophthalmology Retina* (2018), doi: <https://doi.org/10.1016/j.oret.2018.10.012>.

This is a PDF file of an unedited manuscript that has been accepted for publication. As a service to our customers we are providing this early version of the manuscript. The manuscript will undergo copyediting, typesetting, and review of the resulting proof before it is published in its final form. Please note that during the production process errors may be discovered which could affect the content, and all legal disclaimers that apply to the journal pertain.



1 **Predictive Value of the OCT Double-Layer Sign for Identifying Subclinical**
2 **Neovascularization in Age-Related Macular Degeneration**

3
4 Yingying Shi, MD, Elie H. Motulsky, MD, PhD, Raquel Goldhardt, MD, FACS, Yehoshua
5 Zohar, MD, MHA, Marie Thulliez, MD, William Feuer, MS, Giovanni Gregori, PhD, Philip
6 J. Rosenfeld, MD, PhD

7
8 Department of Ophthalmology, Bascom Palmer Eye Institute, University of Miami Miller
9 School of Medicine, Miami, Florida, USA

10
11 **Corresponding Author:**

12 Philip J. Rosenfeld MD, PhD
13 Bascom Palmer Eye Institute
14 900 NW 17th street
15 Miami, FL, 33136
16 Voice: 305-326-6148
17 Fax: 305-326-6538
18 E-mail: prosenfeld@miami.edu

19
20 **Meeting Presentation:** This research will be presented during Retina Subspecialty Day
21 at the American Academy of Ophthalmology Meeting, October 2018.

22
23 **Financial Support:** Research supported by grants from Carl Zeiss Meditec, Inc. (Dublin,
24 CA), the Salah Foundation, an unrestricted grant from the Research to Prevent
25 Blindness, Inc., New York, NY, and the National Eye Institute Center Core Grant
26 (P30EY014801) to the Department of Ophthalmology, University of Miami Miller School
27 of Medicine. The funding organization had no role in the design or conduct of this
28 research.

29
30 **Conflicts of Interest:**

31 Dr. Gregori and Dr. Rosenfeld received research support from Carl Zeiss Meditec, Inc.
32 Dr. Gregori and the University of Miami co-own a patent that is licensed to Carl Zeiss
33 Meditec, Inc. Dr. Rosenfeld also received additional research support from Genentech
34 and Tyrogenex; consultancy for Boehringer-Ingelheim, Carl Zeiss Meditec, Chengdu
35 Kanghong Biotech, Genentech, Healios K.K, F. Hoffmann-La Roche Ltd., Isarna
36 Pharmaceuticals, MacRegen Inc., Ocudyne, Ocunexus Therapeutics, Tyrogenex, and
37 Unity Biotechnology; equity interests in Apellis, Digisight, and Ocudyne.
38 The other authors have no disclosures.

39

40 **Running head:** Identification of subclinical MNV using double layer sign

41

42 **Address for reprints:**

43 Philip J. Rosenfeld, MD, PhD

44 Bascom Palmer Eye Institute,

45 900 NW 17th street,

46 Miami, FL, 33136

47

48 **Abstract**

49 **Purpose:** Structural optical coherence tomography (OCT) images from eyes with non-
50 exudative age-related macular degeneration (AMD) were graded for the presence of a
51 double layer sign to determine if the double-layer sign predicted subclinical macular
52 neovascularization (MNV).

53 **Design:** Prospective, observational study.

54 **Participants:** Non-exudative AMD patients with and without subclinical MNV identified
55 by swept source OCT angiography (SS-OCTA).

56 **Methods:** Subjects were enrolled prospectively into a SS-OCTA imaging study. A set of
57 test scans with and without subclinical MNV was compiled to assess the ability of
58 trained graders to identify non-exudative type 1 MNV. The graders only evaluated the
59 structural OCT B-scans of those eyes. The presence of a double-layer sign was used as
60 a predictive sign for subclinical type 1 MNV. Sensitivity, specificity, positive predictive
61 value (PPV), negative predictive value (NPV) from two separate gradings were
62 calculated and compared.

63 **Main Outcome Measures:** The association between the presence of a double-layer
64 sign and subclinical type 1 MNV.

65 **Results:** One hundred eyes with non-exudative AMD from 94 patients were used for
66 this study. The test set contained 64 eyes with intermediate AMD (iAMD), which
67 included 20 eyes with subclinical MNV, and 36 eyes with late AMD, which included 13
68 eyes with subclinical MNV. Two junior graders read the scans separately then reached
69 a consensus grading. They detected a double-layer sign in 24 out of 33 eyes with
70 subclinical MNV and did not detect a double-layer sign in 56 out of 67 eyes without
71 MNV. Their sensitivity, specificity, PPV, and NPV were 73%, 84%, 69%, and 86%,
72 respectively. The senior grader detected a double-layer sign in 29 out of 33 eyes with
73 subclinical MNV and did not detect a double-layer sign in 58 out of 67 eyes without
74 MNV, achieving a sensitivity, specificity, PPV, and NPV as 88%, 87%, 76%, and 94%,
75 respectively. For all graders, there were statistically significant associations between the
76 type 1 MNV and the double-layer sign ($P < 0.001$).

77 **Conclusions:** The double-layer sign on structural OCT B-scans was associated with
78 subclinical type 1 MNV and can be used to identify these lesions with good predictive
79 values in eyes with non-exudative AMD.

ACCEPTED MANUSCRIPT

80 Introduction

81 Sato et al. were the first to describe the double-layer sign on optical coherence
82 tomography (OCT) B-scans.¹ Using a time domain OCT system (Stratus OCT; Carl
83 Zeiss Meditec, Dublin, CA), they scanned 44 eyes with polypoidal choroidal
84 vasculopathy (PCV) and found two highly reflective layers in 59% of these eyes and
85 these layers corresponded to the regions with branching vascular networks identified by
86 indocyanine green angiography (ICGA). The double-layer sign was comprised of two
87 highly reflective layers that corresponded to a separation between the retinal pigment
88 epithelium (RPE) and another highly reflective layer beneath the RPE, which was
89 presumed to be Bruch's membrane (BM). This double-layer sign represented a low lying,
90 irregular pigment epithelial detachment.

91 In subsequent OCT imaging studies, the double-layer sign was found to
92 correspond to type 1 macular neovascularization (MNV) in eyes with non-exudative
93 age-related macular degeneration (AMD).²⁻⁶ In 2013, Querques et al. observed 11 eyes
94 with non-exudative AMD using multimodal imaging that included fluorescein
95 angiography (FA), ICGA, and spectral-domain OCT (SD-OCT).² The type 1 MNV was
96 visualized using FA and ICGA. Meanwhile, at the site of subclinical MNV, SD-OCT
97 imaging revealed an irregularly, slightly elevated RPE with moderately reflective
98 material in the sub-RPE space that was distinct from the underlying BM layer.

99 The presence of a double-layer sign appears to correlate with the presence of
100 non-exudative type 1 MNV. However, direct visualization of these non-exudative
101 neovascular lesions requires the use of ICGA or OCT angiography (OCTA).⁶⁻¹⁷ It is
102 important to identify these lesions in routine clinical practice since AMD eyes with
103 asymptomatic, subclinical type 1 MNV have a higher annual risk of exudation compared
104 with eyes without these lesions.³ OCTA is a simple, safe, non-invasive strategy for the
105 detection of type 1 MNV, which is much more practical than ICGA for routine screening.
106 Moreover, SS-OCTA provides better visualization of the full extent of the type 1 MNV
107 compared with SD-OCTA imaging.^{3, 4, 10, 18} However, these OCTA instruments are more
108 expensive and not as widely available in clinical practices as the routine structural OCT
109 instruments.

110 In order to determine whether structural OCT images can be used to detect
111 subclinical MNV reliably, this study tests the predictive value of a double-layer sign seen
112 on structural OCT B-scans for the detection of subclinical MNV compared with SS-
113 OCTA imaging in eyes with intermediate and late non-exudative AMD.

114

115 **Material and Methods**

116 Patients with non-exudative AMD were enrolled in a prospective OCT study at
117 Bascom Palmer Eye Institute from April 2016 through January 2018. The institutional
118 review board of the University of Miami Miller School of Medicine approved this study.
119 Informed consent was obtained from all patients. The study was performed in
120 accordance with the tenets of the Declaration of Helsinki and complied with Health
121 Insurance Portability and Accountability Act of 1996.

122 SS-OCTA (PLEX® Elite 9000; Carl Zeiss Meditec, Inc, Dublin, CA) images were
123 acquired using a 6x6 mm scan pattern centered on the fovea. The SS-OCT laser
124 operates at a central wavelength of 1060 nm (1000-1100 nm full width) and a speed of
125 100,000 A-scans per second. At the level of the retina, the full width at half-maximum
126 axial resolution is approximately 5 microns with an estimated lateral resolution at the
127 retinal surface of appropriately 14 microns. In the 6x6 mm scan pattern, a single B scan
128 consisted of 500 A-scans and two B-scans are repeated at each of 500 B-scan
129 positions. *En face* flow images were generated by the instrument using the OCT
130 microangiography (OMAG) algorithm, as previously described.^{17, 19, 20} For the
131 visualization of the MNV, a custom segmentation strategy was used to create slabs
132 extending from the RPE to BM. This feature is available on the commercial instrument
133 and allows the reviewer to select pre-specified boundary layers, and in this study, the
134 boundary layers selected for segmentation were the RPE and the RPE-fit, also known
135 as BM. Obvious artifacts in the boundaries generated by the automated segmentations
136 were corrected using the editing tool.

137 In addition to SS-OCTA, all the patients underwent routine clinical examination.
138 All AMD eyes included in this study had no evidence of exudation based on the
139 absence of macular fluid after review of the retina thickness maps and B-scans from the
140 SSOCT images. Non-exudative AMD eyes were classified by clinical examinations as

141 either intermediate AMD (iAMD) or late AMD.²¹ Eyes with drusen of at least 125 microns
142 in diameter or pigmentary changes, but without evidence of geographic atrophy (GA) or
143 exudation, were defined as iAMD. Late AMD was defined by the presence of GA,
144 defined as complete RPE and outer retinal atrophy (cRORA), in the absence of
145 exudation.²² The diagnosis of subclinical MNV was based on SS-OCTA imaging as
146 previously described.^{3, 4} Eyes with subclinical MNV, which included eyes with both iAMD
147 and late AMD, were chosen based on the knowledge that the graders had not
148 previously evaluated these cases. The eyes without MNV were chosen based on the
149 presence of intermediate or late non-exudative AMD and their clinical characteristics
150 were similar to the eyes with MNV. Eyes with GA, which not fully contained within the
151 6X6 mm scan area were excluded.

152 Three graders (PJR, RG and ZY) graded the study cases without any prior
153 knowledge or review of the cases and whether subclinical MNV was present. Prior to
154 the official grading, the senior grader (PJR) with experience in visualizing MNV on SS-
155 OCTA imaging trained two junior graders (RG and ZY) to recognize double-layer sign
156 using a small training set of cases that were separate from the grading set of cases.
157 The graders only graded whether the B-scans contained a double-layer sign. The
158 double-layer sign term used in this study was characterized by a low-lying irregular RPE
159 detachment with reflective material in sub-RPE space, which was above the highly
160 reflective layer identified as BM. Each grader reviewed the eyes in the validation set, in
161 a random order, using only the *en face* total retina structure image and structural B-
162 scans, but without any flow information. The eyes in the validation set were graded for
163 the presence or absence of a double-layer sign, furthermore the numerical positions of
164 the B-scans corresponding to the double-layer sign was recorded. When there was
165 disagreement between the two junior graders, they were asked to reach a consensus
166 grading.

167 Two sets of gradings, the consensus results from the two junior graders and the
168 one from the senior grader, were analyzed separately and then compared. Sensitivity,
169 specificity, positive predictive value (PPV), and negative predictive value (NPV) of the
170 double-layer sign for identifying subclinical MNV were calculated. Proportions were
171 compared with the Fisher exact test and agreement between ratings was quantified with

172 percent agreement and Cohen's Kappa statistic. Kappa adjusts percent agreement for
173 marginal prevalence and a guide to its interpretation is: < 0.40, poor agreement; > 0.75,
174 excellent agreement; 0.40 to 0.75, fair to good agreement.²³

175

176 **Results**

177 One hundred eyes with non-exudative AMD from 94 patients were graded for the
178 presence of subclinical MNV based on structural OCT information alone (Table 1). Of
179 the 100 eyes enrolled in this study, 64 eyes were in the iAMD group and 36 eyes were
180 in the late AMD group. Of the 64 eyes with iAMD, 20 eyes were diagnosed with
181 subclinical MNV and 44 eyes did not contain subclinical MNV. Of the 36 eyes with late
182 AMD, 13 eyes were diagnosed with subclinical MNV and 23 eyes did not contain
183 subclinical MNV (Table 1).

184 The senior and junior graders agreed on the presence of a double-layer sign in
185 24 eyes out of the 33 eyes with subclinical MNV. In 4 eyes with subclinical MNV, both
186 gradings agreed on the absence of a double-layer sign. There was disagreement
187 between the junior and senior graders on 5 eyes with subclinical MNV (Table 2).

188 The two gradings agreed on the absence of a double-layer sign in 52 out of the
189 67 eyes without subclinical MNV. In 5 eyes without subclinical MNV, both gradings
190 agreed on the presence of a double-layer sign. There was disagreement between the
191 junior and senior graders on 10 eyes without subclinical MNV (Table 2). Agreement
192 between the senior grader and junior graders was excellent for iAMD (% agreement =
193 89%, Kappa=0.761), moderate for advanced AMD (% agreement = 78%, kappa =
194 0.546), and intermediate for all AMD (% agreement = 85%, Kappa=0.677).

195 The sensitivity, specificity, PPV, and NPV of the junior graders were 73%, 84%,
196 69% and 86% respectively. The sensitivity, specificity, PPV and NPV of the senior
197 grader were 88%, 87%, 76% and 94%, respectively. Overall, the association between
198 the double-layer sign and subclinical neovascularization for both gradings was found to
199 be highly statistically significant ($P < 0.001$). However, the two gradings showed that the
200 double-layer sign was a better predictor of subclinical MNV in eyes with drusen ($P <$
201 0.001) than eyes with GA ($P = 0.056$ for the junior grading, $P = 0.001$ for the senior
202 grading) as shown in Table 3.

203 Figure 1 shows two eyes with iAMD and subclinical MNV in which both gradings
204 identified a double-layer sign. SS-OCTA *en face* images show the MNV using a custom
205 slab that extended from the RPE to BM. A color-coded B scan also demonstrates the
206 flow information under the RPE that correlated with the MNV. Structural B scans
207 through the lesion show a typical double-layer sign as a low-lying, irregular elevation of
208 the RPE above BM. Within the sub-RPE space, moderately reflective material is
209 detected. Figure 2 shows examples of two eyes with subclinical MNV in which both
210 gradings did not identify a double-layer sign. SS-OCTA *en face* imaging showed small
211 foci of MNV that corresponded to drusen-like elevations of the RPE seen on B-scans.
212 Figure 3 shows examples in which there was a disagreement between graders as to
213 whether a double-layer sign was present. This disagreement existed even though the B-
214 scans through the MNV showed an apparent double-layer sign. Figure 4 shows two
215 eyes with iAMD in which MNV was not diagnosed based on SS-OCTA *en face* and B-
216 scan flow imaging, yet a double-layer sign was identified. Both gradings identified a
217 double-layer sign in the eye shown in panels A through D. In panels E through H, there
218 was disagreement between the gradings as to whether a double-layer sign was present.
219 Figure 5 shows two eyes with late AMD and subclinical neovascular lesions in which
220 both gradings identified a double-layer sign. SS-OCTA *en face* images show the MNV
221 using a custom slab that extended from the RPE to BM. A color-coded B scan also
222 demonstrates the flow information under the RPE that correlated with the MNV.
223 Structural B scans through the lesion show the double-layer sign that is adjacent to the
224 GA. Figure 6 shows two eyes with late AMD in which MNV was not present based on
225 SS-OCTA *en face* and B-scan flow imaging, yet a double-layer sign was identified. Both
226 gradings identified a double-layer sign in the eye shown in panels A through E. In
227 panels F through J, there was disagreement among the gradings as to whether a
228 double-layer sign was present.

229

230 Discussion

231 Previous OCTA studies have shown that subclinical type 1 MNV corresponded to
232 a double-layer sign on structural OCT B-scans.^{3, 4, 10, 11, 24, 25} However, it was not known
233 if the presence of this double-layer sign on structural OCT images could be used to

234 predict the presence of subclinical neovascularization. In our current study, we used
235 SS-OCTA imaging as the gold standard for the detection of MNV, we found that all the
236 eyes with subclinical MNV did show a double-layer sign, and the graders correctly
237 identified the MNV based on the presence of the double-layer sign seen on structural B-
238 scans in most of these eyes. While the sensitivity and specificity were good, we feel the
239 positive and negative predictive values, which take into account the prevalence of MNV,
240 are more useful.²⁶ These reflect the real world scenarios in which the absolute truth of
241 the presence of MNV is not known and the clinician wants to gauge how likely it is that
242 the presence or absence of a double-layer sign finding predicts the presence or
243 absence of MNV. In this study, the subclinical MNV prevalence was 33%. If in a
244 different clinical setting the prevalence were lower, say 10%, then the senior grader's
245 PPV for the presence of double-layer sign in iAMD would be reduced to 59%, but the
246 NPV for the absence of double-layer sign would increase to 99%.

247 At the beginning of the study, we had assumed that graders would have more
248 difficulty in identifying a double-layer sign in eyes with drusen compared with eyes that
249 had GA, since both drusen and type 1 MNV cause elevations of the RPE. Thus, we
250 expected that the presence of drusen in the eyes with iAMD would be a confounding
251 feature for the graders compared with the presence of GA in late AMD. However, this
252 was not the case. For the most part, graders were able to distinguish typical drusen as
253 focal elevations of the RPE and distinguish these small RPE detachments or focal
254 double-layer signs from the more irregular double-layer sign associated with MNV.
255 While the graders did miss small focal areas of MNV that had configurations similar to
256 drusen, they were better at identifying true double-layer signs associated with MNV in
257 iAMD than in eyes with GA. This came as a surprise. While most MNV in eyes with GA
258 can be found along the margin of the GA, the graders also identified areas at the
259 margins of GA that contained a presumed double-layer sign, but did not contain MNV
260 based on SS-OCTA imaging. This feature of GA, which may be a consequence of the
261 ongoing degeneration of the outer retina and RPE at the margins of the lesions, may be
262 a confounder when assessing for a double-layer sign associated with MNV or may
263 serve as a potential space for the subsequent growth of MNV. Another possibility is that
264 MNV could have been present in these areas with a double-layer sign and just not

265 detected using SS-OCTA imaging. To determine which possibility is likely, ongoing
266 natural history studies using SS-OCTA to follow eyes with late AMD should provide
267 answers.

268 The ability of graders to distinguish typical drusen from a double-layer sign
269 associated with MNV suggests that the differences between these two types of RPE
270 detachments can be easily learned based on certain structural OCT characteristics. The
271 double-layer sign term used in this study was characterized by two highly reflectively
272 layers (RPE and BM) seen on OCT imaging, an irregular contour of the RPE, an
273 elevation with a width usually greater than typical drusen as seen on OCT B-scans, and
274 an internal reflectivity within RPE detachments harboring MNV that appeared different
275 from the reflectivity seen with typical non-vascularized drusen (as showed in Figure 5,
276 panel J). However, there may be other subtler features that are used to distinguish
277 drusen from double-layer signs associated with MNV. The next obvious step would be
278 to try to establish a machine-learning algorithm that might be able to better identify MNV
279 based on the above-mentioned B-scan features and other subtler structural OCT
280 features associated with subclinical type 1 MNV.

281 Previous studies have shown that eyes with chronic central serous
282 chorioretinopathy (CSC) and PCV also contain double layer signs detectable on B-
283 scans, which have been correlated with type 1 MNV.²⁷⁻³⁰ While Bousquet et al.²⁹ found
284 that only one third of these double-layer signs in CSC correlated with type 1 MNV (CNV),
285 Dansingani et al.²⁸ found that in eyes with PCV, the double layer sign was a good
286 diagnostic predictor of a branching vascular network or type 1 MNV. These results may
287 be related to different features of these diseases and different imaging strategies, but
288 the presence of drusen and GA in AMD present their own unique set of challenges.

289 In AMD, the ability to identify subclinical MNV is important when recruiting
290 patients into clinical trials, especially when the outcome of the trial depends on
291 preventing exudation or slowing disease progression.^{31, 32} Whether to exclude such
292 eyes from participation in trials will be at the discretion of the study organizers, but it
293 stands to reason that these subclinical lesions are common and need to be studied.
294 Consequently, we believe these eyes should be included and stratified between groups
295 in a randomized trial. Moreover, subclinical MNV will arise during the course of any

296 AMD trial, so it will be important to detect them and determine if the treatment under
297 study affected their formation or progression to exudation. Therefore, it is important to
298 use OCTA in all AMD trials to identify and monitor these lesions. In the absence of
299 OCTA, our study suggests that reviewing B-scans for the presence of a double-layer
300 sign might suffice, but it is labor intensive, small lesions will be missed, and double-layer
301 signs at the edge of GA might be misinterpreted as MNV. If the aforementioned
302 machine-learning algorithm can be developed to identify subclinical MNV, then it will be
303 a more objective, efficient, and cost-effective way of screening for subclinical MNV in
304 clinical trials where OCTA is not performed. In addition, in clinical practices without
305 OCTA capability, an algorithm capable of identifying subclinical type 1 MNV would be
306 very useful to use in conjunction with routine structural OCT imaging to identify these
307 lesions that are at risk for exudation.

308 A limitation of this study was the use of SS-OCTA as the gold standard for the
309 diagnosis of type 1 MNV. While ICGA is the historical gold standard for the detection of
310 these subclinical lesions, our experience is that SS-OCTA is as good as or better than
311 ICGA for the detection of these lesions.^{2-6, 10, 12, 14, 30, 32} However, it is possible that
312 ICGA might have detected a small subclinical neovascular lesion that was not detected
313 using SS-OCTA, but since ICGA is not routinely performed or reimbursed when used to
314 screen for subclinical MNV in eyes with non-exudative AMD, this limitation isn't clinically
315 relevant since ICGA imaging would not have been performed. Moreover, if SS OCTA
316 were available, then ICGA would be riskier, more time consuming and more expensive
317 for patients with non-exudative AMD. Another limitation of this study is that we used SS
318 OCT images to exclude cases in which subtle leakage might have been detected using
319 fluorescein angiography (FA). Even if FA is the golden standard for detecting leakage
320 from MNV, it is not routinely performed in the absence of intra- or sub-retinal fluid seen
321 on structural OCT imaging. We don't routinely perform FA to detect subtle leakage in
322 the absence of OCT structural changes, and a recent study has shown that FA provides
323 no additional benefit for the management of exudative AMD compared with OCT
324 imaging alone.³³ In the worse case scenario, our study correlates the presence of a
325 double-layer sign seen on structural OCT B-scans with the presence of subclinical MNV
326 detected using SS-OCT angiographic technology. In the best-case scenario, SS-OCTA

327 imaging is the gold standard for the detection of these lesions, and while the
328 correlations between structural B-scans and SS-OCTA images are good, SS-OCTA
329 imaging is superior to structural B-scans for the detection of subclinical MNV.

330 In summary, we found that the double-layer sign on structural OCT B-scans
331 could predict the presence of subclinical MNV in most eyes with non-exudative AMD
332 identified by SS-OCTA imaging. Confirmatory prospective natural history studies of
333 eyes with iAMD and late AMD are ongoing and the development of a machine-learning
334 algorithm to identify subclinical MNV based on structural OCT is underway.

335 **References**

- 336 1. Sato T, Kishi S, Watanabe G, et al. Tomographic features of branching vascular
337 networks in polypoidal choroidal vasculopathy. *Retina* 2007;27(5):589-94.
- 338 2. Querques G, Srour M, Massamba N, et al. Functional characterization and
339 multimodal imaging of treatment-naive "quiescent" choroidal neovascularization. *Invest*
340 *Ophthalmol Vis Sci* 2013;54(10):6886-92.
- 341 3. de Oliveira Dias JR, Zhang Q, Garcia JMB, et al. Natural History of Subclinical
342 Neovascularization in Nonexudative Age-Related Macular Degeneration Using Swept-
343 Source OCT Angiography. *Ophthalmology* 2018;125(2):255-66.
- 344 4. Roisman L, Zhang Q, Wang RK, et al. Optical Coherence Tomography
345 Angiography of Asymptomatic Neovascularization in Intermediate Age-Related Macular
346 Degeneration. *Ophthalmology* 2016;123(6):1309-19.
- 347 5. Capuano V, Miere A, Querques L, et al. Treatment-Naive Quiescent Choroidal
348 Neovascularization in Geographic Atrophy Secondary to Nonexudative Age-Related
349 Macular Degeneration. *Am J Ophthalmol* 2017;182:45-55.
- 350 6. Carnevali A, Cicinelli MV, Capuano V, et al. Optical Coherence Tomography
351 Angiography: A Useful Tool for Diagnosis of Treatment-Naive Quiescent Choroidal
352 Neovascularization. *Am J Ophthalmol* 2016;169:189-98.
- 353 7. Hanutsaha P, Guyer DR, Yannuzzi LA, et al. Indocyanine-green
354 videoangiography of drusen as a possible predictive indicator of exudative maculopathy.
355 *Ophthalmology* 1998;105(9):1632-6.
- 356 8. Guyer DR, Yannuzzi LA, Slakter JS, et al. Classification of choroidal
357 neovascularization by digital indocyanine green videoangiography. *Ophthalmology*
358 1996;103(12):2054-60.
- 359 9. Schneider U, Gelissen F, Inhoffen W, Kreissig I. Indocyanine green angiographic
360 findings in fellow eyes of patients with unilateral occult neovascular age-related macular
361 degeneration. *Int Ophthalmol* 1997;21(2):79-85.
- 362 10. Novais EA, Adhi M, Moulton EM, et al. Choroidal Neovascularization Analyzed on
363 Ultrahigh-Speed Swept-Source Optical Coherence Tomography Angiography
364 Compared to Spectral-Domain Optical Coherence Tomography Angiography. *Am J*
365 *Ophthalmol* 2016;164:80-8.

- 366 11. Lane M, Moulton EM, Novais EA, et al. Visualizing the Choriocapillaris Under
367 Drusen: Comparing 1050-nm Swept-Source Versus 840-nm Spectral-Domain Optical
368 Coherence Tomography Angiography. *Invest Ophthalmol Vis Sci* 2016;57(9):OCT585-
369 90.
- 370 12. Miller AR, Roisman L, Zhang Q, et al. Comparison Between Spectral-Domain
371 and Swept-Source Optical Coherence Tomography Angiographic Imaging of Choroidal
372 Neovascularization. *Invest Ophthalmol Vis Sci* 2017;58(3):1499-505.
- 373 13. Zhang Q, Zhang A, Lee CS, et al. Projection artifact removal improves
374 visualization and quantitation of macular neovascularization imaged by optical
375 coherence tomography angiography. *Ophthalmol Retina* 2017;1(2):124-36.
- 376 14. Nehemy MB, Brocchi DN, Veloso CE. Optical Coherence Tomography
377 Angiography Imaging of Quiescent Choroidal Neovascularization in Age-Related
378 Macular Degeneration. *Ophthalmic Surg Lasers Imaging Retina* 2015;46(10):1056-7.
- 379 15. Palejwala NV, Jia Y, Gao SS, et al. Detection of Nonexudative Choroidal
380 Neovascularization in Age-Related Macular Degeneration with Optical Coherence
381 Tomography Angiography. *Retina* 2015;35(11):2204-11.
- 382 16. Huang Y, Zhang Q, Thorell MR, et al. Swept-source OCT angiography of the
383 retinal vasculature using intensity differentiation-based optical microangiography
384 algorithms. *Ophthalmic Surg Lasers Imaging Retina* 2014;45(5):382-9.
- 385 17. Wang RK, An L, Francis P, Wilson DJ. Depth-resolved imaging of capillary
386 networks in retina and choroid using ultrahigh sensitive optical microangiography. *Opt*
387 *Lett* 2010;35(9):1467-9.
- 388 18. Zhang Q, Chen CL, Chu Z, et al. Automated Quantitation of Choroidal
389 Neovascularization: A Comparison Study Between Spectral-Domain and Swept-Source
390 OCT Angiograms. *Invest Ophthalmol Vis Sci* 2017;58(3):1506-13.
- 391 19. Zhang A, Zhang Q, Chen CL, Wang RK. Methods and algorithms for optical
392 coherence tomography-based angiography: a review and comparison. *J Biomed Opt*
393 2015;20(10):100901.
- 394 20. Yin X, Chao JR, Wang RK. User-guided segmentation for volumetric retinal
395 optical coherence tomography images. *J Biomed Opt* 2014;19(8):086020.

- 396 21. Ferris FL, 3rd, Wilkinson CP, Bird A, et al. Clinical classification of age-related
397 macular degeneration. *Ophthalmology* 2013;120(4):844-51.
- 398 22. Schaal KB, Rosenfeld PJ, Gregori G, et al. Anatomic Clinical Trial Endpoints for
399 Nonexudative Age-Related Macular Degeneration. *Ophthalmology* 2016;123(5):1060-79.
- 400 23. Fleiss JL. *Statistical methods for rates and proportions*. 2nd ed. New York, NY:
401 John Wiley & Sons; 1981 1981:Pp 212-25.
- 402 24. Moulton E, Choi W, Waheed NK, et al. Ultrahigh-speed swept-source OCT
403 angiography in exudative AMD. *Ophthalmic Surg Lasers Imaging Retina*
404 2014;45(6):496-505.
- 405 25. Zhang A, Zhang Q, Wang RK. Minimizing projection artifacts for accurate
406 presentation of choroidal neovascularization in OCT micro-angiography. *Biomed Opt*
407 *Express* 2015;6(10):4130-43.
- 408 26. Fleiss JL. *Statistical Methods for Rates and Proportions*. 2nd ed. New York, NY:
409 John Wiley and Sons; 1981 1981:Pp 4-8.
- 410 27. Hage R, Mrejen S, Krivosic V, et al. Flat irregular retinal pigment epithelium
411 detachments in chronic central serous chorioretinopathy and choroidal
412 neovascularization. *Am J Ophthalmol* 2015;159(5):890-903 e3.
- 413 28. Dansingani KK, Balaratnasingam C, Klufas MA, et al. Optical Coherence
414 Tomography Angiography of Shallow Irregular Pigment Epithelial Detachments In
415 Pachychoroid Spectrum Disease. *Am J Ophthalmol* 2015;160(6):1243-54 e2.
- 416 29. Bousquet E, Bonnin S, Mrejen S, et al. Optical Coherence Tomography
417 Angiography of Flat Irregular Pigment Epithelium Detachment in Chronic Central Serous
418 Chorioretinopathy. *Retina* 2018;38(3):629-38.
- 419 30. Inoue M, Jung JJ, Balaratnasingam C, et al. A Comparison Between Optical
420 Coherence Tomography Angiography and Fluorescein Angiography for the Imaging of
421 Type 1 Neovascularization. *Invest Ophthalmol Vis Sci* 2016;57(9):OCT314-23.
- 422 31. Maguire MG, Daniel E, Shah AR, et al. Incidence of choroidal neovascularization
423 in the fellow eye in the comparison of age-related macular degeneration treatments
424 trials. *Ophthalmology* 2013;120(10):2035-41.

- 425 32. Barbazetto IA, Saroj N, Shapiro H, et al. Incidence of new choroidal
426 neovascularization in fellow eyes of patients treated in the MARINA and ANCHOR trials.
427 Am J Ophthalmol 2010;149(6):939-46 e1.
- 428 33. Parekh PK, Folk JC, Gupta P, et al. Fluorescein Angiography Does Not Alter the
429 Initial Clinical Management of Choroidal Neovascularization in Age-Related Macular
430 Degeneration. Ophthalmology Retina 2018;2(7):659-66.
- 431

432 **FIGURE LEGENDS**

433 **Figure 1:** Two eyes with intermediate age-related macular degeneration (AMD) and
434 subclinical macular neovascularization (MNV) where all graders agreed on the presence
435 of the double layer sign on structural B-scan images. A, E: 6x6 mm *en face*
436 angiographic image of MNV from a slab with segmentation boundaries extending from
437 the retinal pigment epithelium (RPE) to Bruch's membrane (BM) showing CNV pattern;
438 B, F: 6x6 mm *en face* structural images using the same slab as in panels A and E; C, G:
439 OCT structural B-scans through the subclinical type 1 MNV with color-coded flow using
440 red for the retinal microvasculature and green for flow under the RPE. Yellow dashed
441 lines represent the slab boundaries from the RPE to BM. D, H: OCT structural B-scans
442 through the lesion showing a double layer sign (yellow arrow).

443
444 **Figure 2:** Two eyes with late age-related macular degeneration (AMD) and subclinical
445 macular neovascularization (MNV) where none of the graders identified a double layer
446 sign. A, E: 6x6 mm *en face* angiographic image of MNV from a slab with segmentation
447 boundaries extending from the retinal pigment epithelium (RPE) to Bruch's membrane
448 (BM) showing small foci of CNV pattern; B, F: 6x6 mm *en face* structural images using
449 the same slab as in panels A and E; C, G: OCT structural B-scans through the
450 subclinical type 1 MNV with color-coded flow using red for the retinal microvasculature
451 and green for flow under the RPE. Yellow dashed lines represent the slab boundaries
452 from the RPE to BM. D, H: OCT structural B-scans through the lesion showing small
453 elevation of RPE (yellow arrow).

454
455 **Figure 3:** Two eyes with late age-related macular degeneration (AMD) and subclinical
456 macular neovascularization (MNV) where some graders did not identify a double layer
457 sign. A, E: 6x6 mm *en face* angiographic image of MNV from a slab with segmentation
458 boundaries extending from the retinal pigment epithelium (RPE) to Bruch's membrane
459 (BM) showing CNV pattern; B, F: 6x6 mm *en face* structural images using the same
460 slab as in panels A and E; C, G: OCT structural B-scans through the subclinical type 1
461 MNV with color-coded flow using red for the retinal microvasculature and green for flow
462 under the RPE. Yellow dashed lines represent the slab boundaries from the RPE to BM.

463 D, H: OCT structural B-scans through the lesion showing a double layer sign (yellow
464 arrow).

465

466 **Figure 4:** Two eyes with intermediate age-related macular degeneration (AMD) without
467 macular neovascularization (MNV). A – D shows one eye in which all the graders
468 identified the presence of a double layer sign; E – H shows one eye in which junior and
469 senior graders did not reach an agreement as to whether a double layer sign was
470 present. A, E: 6x6 mm *en face* angiographic image using a slab with segmentation
471 boundaries extending from the retinal pigment epithelium (RPE) to Bruch's membrane
472 (BM) showing no CNV pattern; B, F: 6x6 mm *en face* structural images using the same
473 slab as in panels A and E; C, G: OCT structural B-scans with color-coded flow using red
474 for the retinal microvasculature and green for flow under the RPE. Yellow dashed lines
475 represent the slab boundaries from the RPE to BM. D, H: OCT structural B-scans
476 showing double layer sign (yellow arrow).

477

478 **Figure 5:** Two eyes with late age-related macular degeneration (AMD) and subclinical
479 macular neovascularization (MNV) where all graders agreed on the presence of the
480 double layer sign on structural B-scan images. A, F: 6x6 mm *en face* structure image
481 using a slab with segmentation boundaries extending from 64 microns to 400 microns
482 under Bruch's membrane (BM) showing geographic atrophy (GA); B, G: 6x6 mm *en*
483 *face* angiographic image using a slab with segmentation boundaries extending from the
484 retinal pigment epithelium (RPE) to BM showing CNV pattern; C, H: 6x6 mm *en face*
485 structural images using the same slab as in panels B and G; D, I: OCT structural B-
486 scans through the subclinical type 1 MNV with color-coded flow using red for the retinal
487 microvasculature and green for flow under the RPE. Yellow dashed lines represent the
488 slab boundaries from the RPE to BM. E, J: OCT structural B-scans through the lesion
489 showing double layer sign adjacent to GA (yellow arrow).

490

491 **Figure 6:** Two eyes with late age-related macular degeneration (AMD) and evidence of
492 double layer signs on structural B-scans, but no evidence of subclinical macular
493 neovascularization (MNV) on swept-source optical coherence tomography angiography

494 (SS-OCTA). A – D shows one eye in which all the graders incorrectly identified as
495 subclinical MNV based on the presence of double layer sign; E – H shows one eye in
496 which junior and senior graders did not reach an agreement as to whether a double
497 layer sign was present. A, F: 6x6 mm *en face* structure image using a slab with
498 segmentation boundaries extending from 64 microns to 400 microns under Bruch's
499 membrane (BM) showing geographic atrophy (GA); B, G: 6x6 mm *en face* angiographic
500 image showing no CNV pattern using a slab with segmentation boundaries extending
501 from the retinal pigment epithelium (RPE) to BM; C, H: 6x6 mm *en face* structural
502 images using the same slab as in panels B and G; D, I: OCT structural B-scans with
503 color-coded flow using red for the retinal microvasculature and green for flow under the
504 RPE. Yellow dashed lines represent the slab boundaries from the RPE to BM. E, J:
505 OCT structural B-scans showing double layer sign adjacent to GA (yellow arrow).
506

Table 1: Presence of subclinical macular neovascularization in test eyes with non-exudative age-related macular degeneration

Group	Intermediate AMD N = 64	Late AMD N = 36
Presence of subclinical MNV N = 33	20	13
Absence of subclinical MNV N = 67	44	23

MNV = macular neovascularization; AMD = age-related macular degeneration

Table 2: Identification of a double layer sign in test eyes with non-exudative age-related macular degeneration

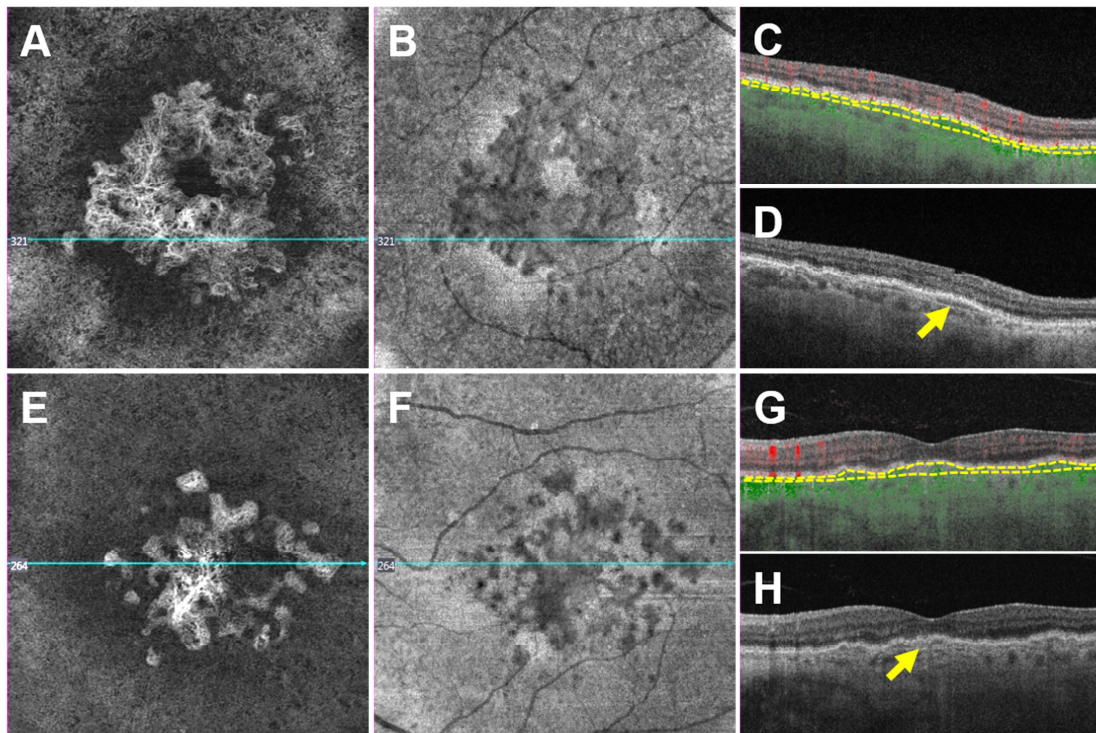
Group	Double layer sign present for junior and senior graders	Double layer sign absent for junior and senior graders	No agreement between junior and senior graders
Presence of Subclinical MNV N = 33	24	4	5
Absence of Subclinical MNV N = 67	5	52	10

MNV = macular neovascularization

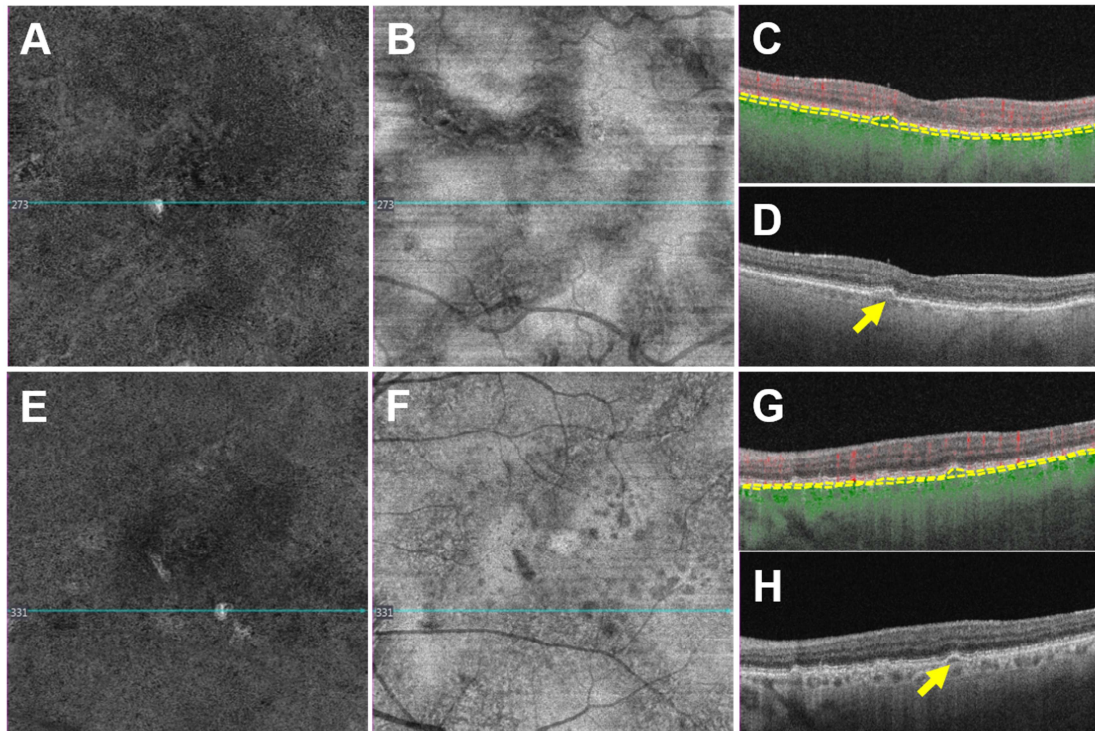
Table 3: Sensitivity, specificity, and predictive values of double layer sign for identifying subclinical macular neovascularization in non-exudative age-related macular degeneration

Values	AMD N = 100		Intermediate AMD N = 64		Late AMD N = 36	
	Consensus from junior graders	Results from senior grader	Consensus from junior graders	Results from senior grader	Consensus from junior graders	Results from senior grader
Sensitivity	24/33 (73%)	29/33 (88%)	17/20 (85%)	18/20 (90%)	7/13 (54%)	11/13 (85%)
Specificity	56/67 (84%)	58/67 (87%)	37/44 (84%)	41/44 (93%)	19/23 (83%)	17/23 (74%)
PPV	24/35 (69%)	29/38 (76%)	17/24 (71%)	18/21 (86%)	7/11 (64%)	11/17 (65%)
NPV	56/65 (86%)	58/62 (94%)	37/40 (93%)	41/43 (95%)	19/25 (76%)	17/19 (89%)
P-value	<0.001	<0.001	<0.001	<0.001	0.056	0.001

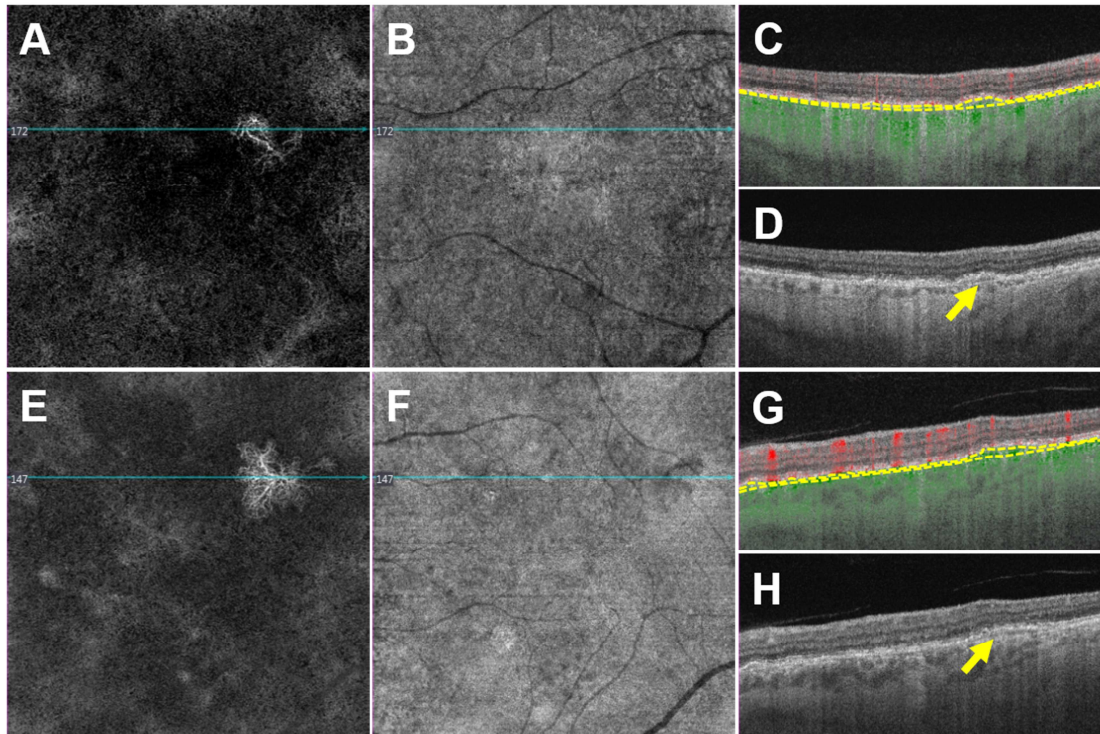
AMD = age-related macular degeneration; PPV = positive predictive value; NPV = negative predictive value



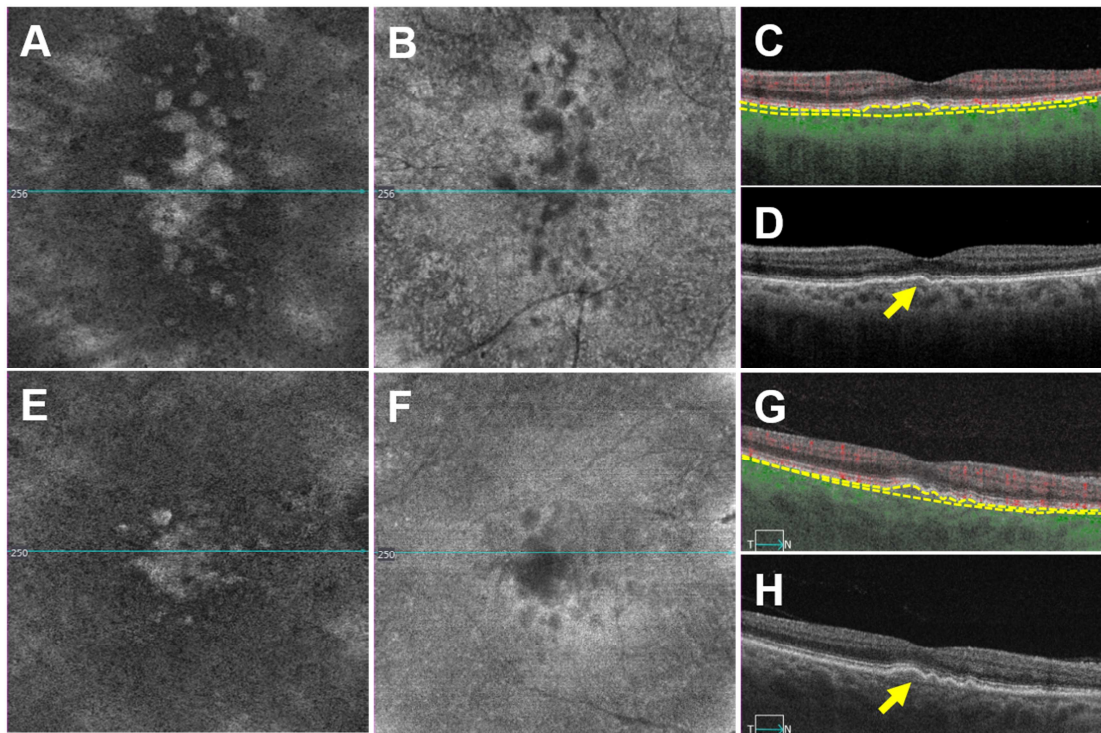
ACCEPTED MANUSCRIPT

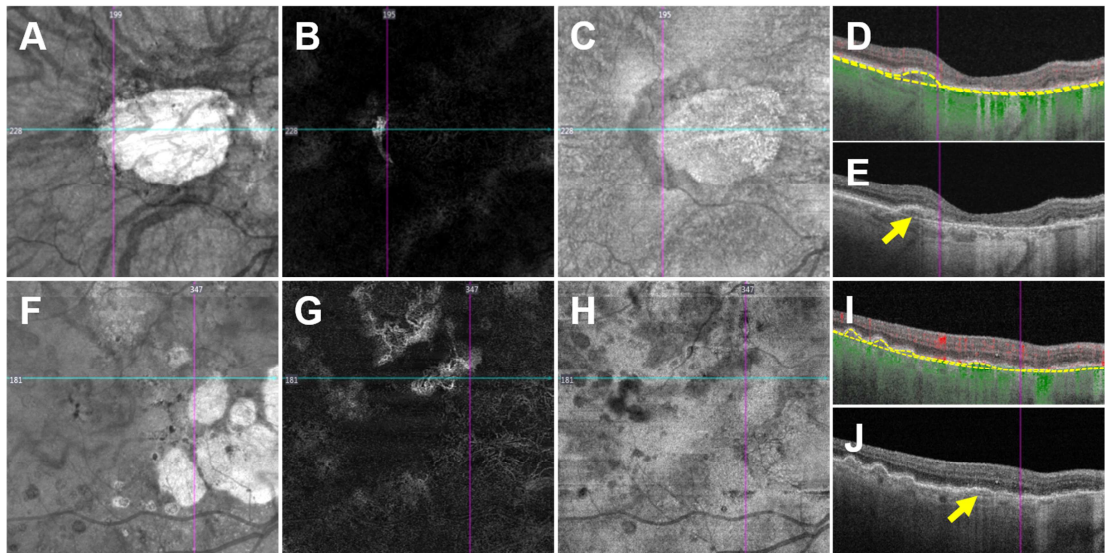


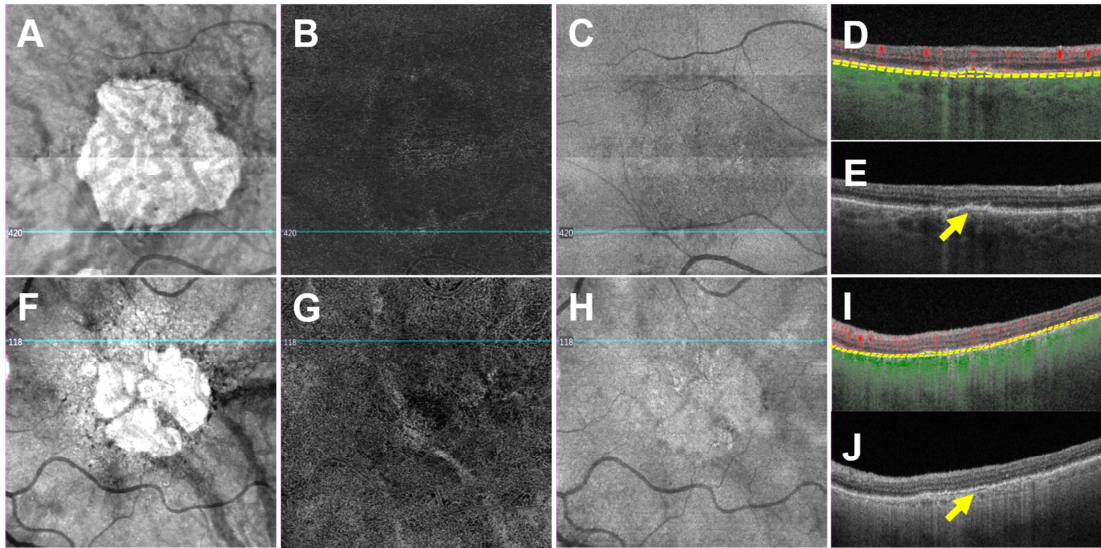
ACCEPTED MANUSCRIPT



ACCEPTED MANUSCRIPT







ACCEPTED MANUSCRIPT

Précis

The double layer sign seen on structural OCT B-scans can predict the presence of subclinical type 1 macular neovascularization in non-exudative age-related macular degeneration, but swept source OCT angiography is better at identifying these lesions.

ACCEPTED MANUSCRIPT